

One-Dimensional Assembling of Diiodo[phthalocyaninato(1–)] Chromate(III) Molecules through Neutral I₂ Molecules. Alternating Ferro- and Antiferromagnetic Interactions in the Metal–Radical System

Jan Janczak*^{†,‡} and Ynara Marina Idemori[†]

Instituto de Ciências Exatas, Departamento de Química, Universidade Federal de Minas Gerais, CEP 31270-901 Belo Horizonte—MG, Brazil, and Institute of Low Temperature and Structure Research, Polish Academy of Sciences, 50-950 Wrocław, P.O. Box 1410, Poland

Received April 3, 2002

Crystals of diiodo[phthalocyaninato(1–)] chromate(III) diiodine, CrPcI₂·I₂, were grown directly in the reaction of chromium powder with 1,2-dicyanobenzene under a stream of iodine at about 250 °C. The CrPcI₂·I₂ complex crystallizes in the centrosymmetric space group of the triclinic system with one molecule per unit cell, with the cell dimensions $a = 7.851(2)$ Å, $b = 8.402(2)$ Å, $c = 12.668(3)$ Å, $\alpha = 80.32(3)^\circ$, $\beta = 74.06(3)^\circ$, $\gamma = 82.33(3)^\circ$, and $V = 788.7(3)$ Å³. The X-ray single-crystal analysis shows that each of the centrosymmetric CrPcI₂ molecules is bridged by a neutral I₂ molecule (detected also by Raman spectroscopy) and develops a polymeric one-dimensional structure. The magnetic measurements have been carried out in the temperature range 300–2 K. Temperature dependence of the effective magnetic moment, μ_{eff} , shows the ferro- and antiferromagnetic interactions in the system of the paramagnetic central Cr³⁺ ion and surrounding π -conjugated radical ligand Pc(1–). The conductivity measurement on a polycrystalline sample exhibits weak temperature dependence ($d\sigma/dT < 0$). The UV–vis spectrum exhibits, besides the B- and Q-bands, one additional band assigned to the electronic transition from a deeper level to the half-occupied HOMO level in the one-electron oxidized phthalocyaninato(1–) radical ligand.

Introduction

Coordination metal complexes with one-dimensional superstructure have received considerable attention in the past two decades.^{1–3} Molecular-based ferromagnets, semiconductors and conductors, and nonlinear optical materials represent several applications of one-dimensional coordination polymers.^{4–10}

Among the numerous and extensive studies on metallophthalocyanines, the iodine-doped metallophthalocyanines and diphthalocyanines with a nonintegral oxidation state of the phthalocyaninato macroring and with pseudo-one-dimensional stacked structure represent materials with high conductivity.^{11–14} In these materials, the iodine-doped atoms form chains of disordered symmetrical triiodide ions that are located in the channels between the pseudo-one-dimensional

* Corresponding author. E-mail: jjanek@dedalus.lcc.ufmg.br.

[†] Universidade Federal de Minas Gerais.

[‡] Polish Academy of Sciences.

- (1) Schneider, O.; Hanack, M. *Angew. Chem., Int. Ed. Engl.* **1982**, *21*, 79.
- (2) Hanack, M.; Deger, S.; Lange, A. *Coord. Chem. Rev.* **1983**, *83*, 115–136.
- (3) Chen, C. T.; Suslick, K. S. *Coord. Chem. Rev.* **1993**, *128*, 293–322.
- (4) Ealton, D. *Science* **1991**, *253*, 281–287.
- (5) *Magnetic Molecular Materials*; Gatteschi, D., Kahn, O., Miller, J. S., Palacio, F., Eds.; NATO ASI Series E; Kluwer: Dordrecht, The Netherlands, 1991; Vol. 198.
- (6) Liang-Fu, T.; Lei, Z.; Li-Chun, L.; Peng, Ch.; Zhi-Hong, W.; Ji-Tao, W. *Inorg. Chem.* **1999**, *38*, 6326–6328.
- (7) Costillo, O.; Lague, A.; Sertucha, J.; Roman, P.; Lioret, F. *Inorg. Chem.* **2000**, *39*, 6142–6144.
- (8) *Extended Linear Chain Compounds*; Miller, J. S., Ed.; Plenum Press: New York, 1982, Vol.3.

- (9) *Organic and Inorganic Linear Dimensional Crystalline Materials*; Dalhes, P., Drillon, M., Eds.; NATO ASI Series 168; NATO: New York, 1989.
- (10) Cortes, R.; Drillon, M.; Solans, X.; Lezama, L.; Rojo, T. *Inorg. Chem.* **1997**, *36*, 677–683.
- (11) Ibers, J. A.; Pace, L. J.; Martinsen, J.; Hoffman, B. M. *Struct. Bonding (Berlin)* **1982**, *50*, 1–55.
- (12) Wynne, K. J.; Nohr, R. S. *Mol. Cryst. Liq. Cryst.* **1982**, *82*, 243–254.
- (13) Martinsen, J.; Greene, R. L.; Palmer, S. L.; Hoffman, B. M. *J. Am. Chem. Soc.* **1983**, *105*, 677–678.
- (14) (a) Janczak, J.; Kubiak, R.; Hahn, F. *Inorg. Chim. Acta* **1998**, *281*, 195–200. (b) Janczak, J.; Kubiak, R. *Polyhedron* **1999**, *18*, 1621–1627. (c) Janczak, J.; Kubiak, R.; Jezierski, A. *Inorg. Chim. Acta* **1999**, *38*, 2043–2049. (d) Janczak, J.; Kubiak, R.; Svoboda, I.; Jezierski, A.; Fuess, H. *Inorg. Chim. Acta* **2000**, *304*, 150–155. (e) Janczak, J.; Idemori, Y. M. *Inorg. Chim. Acta* **2001**, *325*, 85–93.

partially oxidized metallo mono- or diphthalocyaninato ($\text{MPC}^{\delta+}$, $\text{MPC}_2^{\delta+}$) aggregates. Theoretical and experimental investigations of these iodine-doped phthalocyaninato complexes suggested two pathways for the charge transport. The high conductivity of these materials can be explained by (1) a concept of organic molecular metals with charge propagation through $p-\pi$ orbitals of the macrocyclic rings¹⁵ and (2) by linear-chain-metal-spine conductors with charge transport through the metal-based $a_{1g}(d_z^2)$ orbitals.¹⁶

Continuing our investigations in the synthesis and characterization of metallophthalocyanines in the oxidative conditions, under a stream of iodine, we have obtained several iodine-doped metallophthalocyanines.¹⁴ Quite recently, we reported that the iodine-doped atoms in the crystals of metallophthalocyanines can form an ordered but unsymmetrical triiodide ion, as found in MoOPcI_3 ,¹⁷ SbPcI_3 ,¹⁸ and AsPcI_3 ,¹⁹ as well as can be directly joined to the central metal ion yielding mono- or diiodometallophthalocyaninato complexes.^{20,21} Herein, we report the synthesis and investigation of a new one-dimensional polymer of diiodo[phthalocyaninato(1-)] chromate(III) diiodide, $\{\text{CrPcI}_2 \cdot \text{I}_2\}_n$, in which the magnetic transition metal ion (Cr^{3+} , with d^3 configuration) is coordinated by a π -conjugated radical ligand, $\text{Pc}(1^{\cdot-})$.

Experimental Section

Synthesis. All reagents were of the highest grade commercially available and were used as received. The crystals of $\text{CrPcI}_2 \cdot \text{I}_2$ were obtained directly by the reaction of the pure powdered chromium and 1,2-dicyanobenzene under a stream of iodine. The powdered chromium, 1,2-dicyanobenzene, and iodine in a molar proportion of 1:4:4, with about 10% excess of iodine, were mixed together and pressed into pellets. The pellets were inserted into an evacuated glass ampule and sealed. The ampule was heated at 250 °C for 10 h. At this temperature (250 °C), the liquid 1,2-dicyanobenzene undergoes catalytic tetramerization forming the phthalocyaninato macroring, which accepts the electrons from chromium. Simultaneously, the iodine atoms coordinate to the chromium forming the CrPcI_2 complex, which interacts with the iodine molecules yielding good quality black-violet single crystals of $\text{CrPcI}_2 \cdot \text{I}_2$ (Scheme 1). The elemental analysis has been carried out on an energy dispersive spectrometer. Found: C, 35.62; N, 10.34; Cr, 4.84; I, 47.72; H, 1.48%. Calcd for $\text{C}_{32}\text{H}_{16}\text{N}_8\text{CrPcI}_4$: C, 35.85; N, 10.45; Cr, 4.85; I, 47.35; H, 1.50%.

X-ray Crystallography. The X-ray single-crystal data were collected on a Siemens P4 diffractometer equipped with graphite-monochromatized $\text{Mo K}\alpha$ radiation ($\lambda = 0.71073 \text{ \AA}$) and a crystal of size $0.22 \times 0.16 \times 0.12 \text{ mm}^3$. The crystallographic data,

Scheme 1

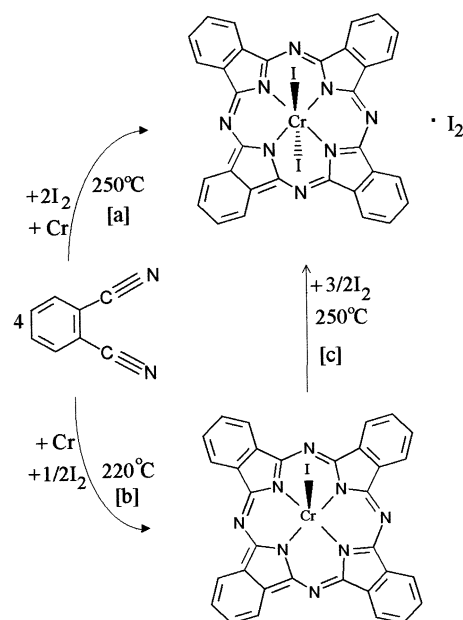


Table 1. Crystallographic Data and Final Refinement Parameters for $\text{CrPcI}_2 \cdot \text{I}_2$

chemical formula	$\text{C}_{42}\text{H}_{26}\text{N}_{10}\text{CrI}_4$
MW	1072.13
temp/°C	22(2)
cryst syst	triclinic
space group	$P\bar{1}$ (No. 2)
unit cell dimensions	
$a/\text{\AA}$	7.851(2)
$b/\text{\AA}$	8.402(2)
$c/\text{\AA}$	12.668(3)
α/deg	80.32(3)
β/deg	74.06(3)
γ/deg	82.33(3)
$V/\text{\AA}^3$	1072.13
Z	1
D_{obsd} (measured by flotation)/ g cm^{-3}	2.25
$D_{\text{calcd}}/\text{g cm}^{-3}$	2.257
radiation, $\text{Mo K}\alpha/\text{\AA}$	0.71073
abs coeff, μ/mm^{-1}	4.315
refinement on F^2	
$R^a [F^2 > 2\sigma(F^2)]$	0.0387
$R_w^b (F^2 \text{ all reflections})$	0.0499
GOF, S	1.007
residual electron density, $\Delta\rho_{\text{max}}, \Delta\rho_{\text{min}}/\text{e \AA}^{-3}$	+0.628, -0.828

$$^a R = \sum ||F_o| - |F_c|| / \sum F_o. \quad ^b R_w = \{ \sum [w(F_o^2 - F_c^2)^2] / \sum wF_o^4 \}^{1/2}; \quad w^{-1} = \sigma^2(F_o^2) + (0.0100P)^2 \quad \text{where } P = (F_o^2 + 2F_c^2)/3.$$

conditions for the collection of intensity data, and some features of the structure refinement parameters are listed in Table 1. Cell parameters were determined by the least-squares methods based on 38 reflections with θ ranging from 5° to 12.80° at 295(2) K.²² A total of 7112 reflections (3644 independent, $R_{\text{int}} = 0.0190$) were measured up to $2\theta = 56^\circ$. Two standard reflections were monitored after every 50. The intensity variation was 0.85%. Face-indexed analytical absorption was calculated using the SHELXTL program.²³ The structure was solved by the Patterson heavy-atom method and refined by the full-matrix least-squares method using the SHELXL-

- (15) (a) Wudl, F. *Acc. Chem. Res.* **1984**, *17*, 227–232. (b) Williams, J. M.; Beno, M. A.; Wang, H. H.; Leung, P. C. W.; Emge, T. J.; Geiser, U.; Carlson, K. D. *Acc. Chem. Res.* **1985**, *18*, 261–267.
- (16) In *One-dimensional organometallic materials: Lecture Notes in Chemistry*, 45; Bohm, M. C., Ed.; Springer-Verlag: Berlin, 1987.
- (17) Janczak, J.; Kubiak, R. *Inorg. Chim. Acta* **1999**, *38*, 2429–2433.
- (18) Kubiak, R.; Janczak, J.; Razik, M. *Inorg. Chim. Acta* **1999**, *293*, 155–159.
- (19) Janczak, J.; Idemori, Y. M. *Acta Crystallogr.* **2002**, *E58*, m36–m38.
- (20) (a) Janczak, J.; Kubiak, R. *Inorg. Chim. Acta* **1999**, *288*, 174–180. (b) Janczak, J.; Idemori, Y. M. *Acta Crystallogr.* **2001**, *C57*, 924–925. (c) Ejsmont, K.; Kubiak, R. *Acta Crystallogr.* **1998**, *C54*, 1844–1846.
- (21) (a) Janczak, J.; Kubiak, R. *Pol. J. Chem.* **1999**, *73*, 1587–1592. (b) Janczak, J.; Kubiak, R. *Acta Crystallogr.* **2001**, *C57*, 55–57. (c) Ejsmont, K.; Kubiak, R. *Acta Crystallogr.* **1997**, *C53*, 1051–1054.

(22) XSCANS; Siemens Analytical X-ray Instrument, Inc.: Madison, WI, 1991.

(23) Sheldrick, G. M. *SHELXTL Program*; Siemens Analytical X-ray Instrument, Inc.: Madison, WI, 1991.

Table 2. Selected Bond Lengths (Å) and Angles (deg) for CrPcI₂·I₂

Cr–N1	1.969(4)
Cr–N3	1.965(4)
Cr–I1	2.750(1)
I1–I2	3.502(1)
I2–I2 ^{ia}	2.773(1)
N–Cr–N3	90.52(15)
N1–Cr–N3 ⁱⁱ	89.48(15)
I1–Cr–N1	90.00(10)
I1–Cr–N3	88.88(10)
I1–Cr–N3 ⁱⁱ	91.12(10)
I1–I2–I2 ⁱ	172.28(3)

^a Symmetry code: (i) $-1 - x, -y, 1 - z$; (ii) $-x, -y, -z$.

97 program²⁴ with anisotropic thermal parameters for all non-hydrogen atoms (for H atoms the $U_{iso} = 1.2U_{iso}$, i.e., 20% higher than the carbon atom directly bonded the H atom). The final difference Fourier maps showed no peaks of chemical significance. Selected bond lengths and angles are summarized in Table 2.

UV–Vis Spectroscopy. Measurements of the electronic spectra of CrPcI₂·I₂ were carried out at room temperature using a Cary–Varian 2300 spectrometer. The UV–vis spectra were recorded from solution in CH₂Cl₂, DMSO, and pyridine in a 0.5 cm quartz cell.

Raman Spectroscopy. The Raman spectrum was recorded at room temperature on a Jobin–Yvon Ramanor U-1000 spectrometer equipped with a photomultiplier-type detector and phonon-counting hardware. The 90° geometry was used. An argon-ion laser line at 514.5 nm at 100 mW power was used as exciting radiation. Resolution was set up to 3 cm⁻¹.

Magnetic Susceptibility Measurement. Magnetic susceptibility measurement of CrPcI₂·I₂ was carried out on a polycrystalline sample in the temperature range 2–300 K with a Quantum Design SQUID magnetometer (San Diego, CA). The susceptometer was calibrated with (NH₄)₂Mn(SO₄)₂·12H₂O. Data were recorded at the magnetic field of 0.5 T on a sample of 50 mg.

Electron Paramagnetic Resonance Measurements. EPR measurements were made on SE-Radiopan and ESR 300E-Bruker X-band spectrometers at room temperature. The studies were carried out on solid samples of 2–5 mg. The concentrations of the free radicals in the samples of CrPcI₂·I₂ were calculated using standard integration of the derivative signal and by comparing the area with the area determined with the free radical standards (DPPH, TEMPO, TEMPOL, and Rickitt’s ultramarine were used as standards). Two EPR lines, one sharp strong signal at $g = 2.0020$ with a bandwidth of $\Gamma = 4.5$ G, the second broader signal at $g \approx 1.96$ ($\Gamma \approx 15$ G), were observed.

Conductivity Measurements. Conductivity measurements were carried out on the polycrystalline compacted samples (pressed into pellets $\sim 10^5$ kPa) by using a standard four-point probe technique²⁵ with a sampling current of 20 μ A. Variation of the temperature was achieved by placing the samples in a cold-gas stream (N₂ or He).

Results and Discussion

Synthesis and Characterization. Our preparation method for the CrPcI₂·I₂ complex is fast and simple. Additionally, this method leads to good quality single crystals. The crystals have been directly obtained from pure powdered chromium

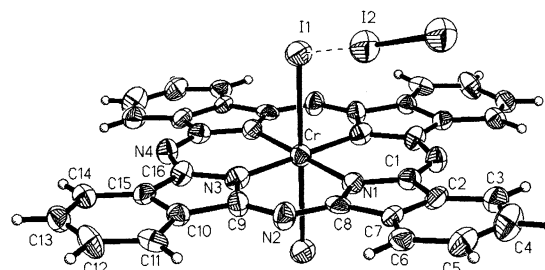


Figure 1. View of the CrPcI₂·I₂ molecule with labeling scheme. Displacement ellipsoids are shown at the 50% probability level.

and phthalonitrile under a stream of iodine at 250 °C (see Scheme 1a). Earlier, we reported that the reaction of powdered chromium with phthalonitrile and iodine used in the molar proportion of 1:4:1 and at lower temperature (~ 220 °C) yields the crystals of CrPcI (Scheme 1b).^{20b} The CrPcI₂·I₂ complex at this temperature (~ 220 °C) could not be obtained; thus, we suppose that the higher temperature (250 °C) is conducive to formation of this complex. The CrPcI₂·I₂ complex could be also obtained from CrPcI under an iodine stream at ~ 250 °C (Scheme 1c) but only in powdered form (identified by elemental analysis and X-ray powder diffraction experiment). The CrPcI₂·I₂ complex is not soluble in water, methanol, or ethanol and is slightly soluble in DMF, DMSO, pyridine, and other aromatic solvent like chloronaphthalene or quinoline. However, after several days in solution, black powder material was obtained. The elemental analysis of this powder material is consistent with the composition of CrPcI₂. Thus, in the solution, the decomposition process of the CrPcI₂·I₂ complex into CrPcI₂ and I₂ takes place. The decomposition of this complex depends strongly on the temperature, and it takes place several times quicker in hot solvents. Because the structural investigation and electrical conductivity measurements for the CrPcI₂ complex, the chloro analogue of the CrPcI₂ complex, are available,²⁶ we also attempted to obtain single crystals of CrPcI₂ suitable for X-ray analysis; however, it was unsuccessful. Contact of the CrPcI₂·I₂ complex with dilute acid leads to demetalation yielding the α -form of metal-free phthalocyanine (α -H₂Pc)²⁷ and appropriate salt.

Description of the Structure. The crystal of CrPcI₂·I₂ is built up from centrosymmetric CrPcI₂ molecules and neutral I₂ molecules (Figure 1). The central metal cation (Cr³⁺) is six-coordinated by four isoindole nitrogen atoms of the one-electron oxidized phthalocyaninato(1–) macrocyclic radical ligand and by two iodine atoms (in trans position) in an octahedral geometry. The tetradentate phthalocyanonato(1–) ligand is not strictly planar. The two opposite isoindole moieties are displaced below the other two above the weighted plane defined by the four isoindole nitrogen atoms (required by the inversion center). The largest deviations (without the H-atoms) from the N₄-isoindole planes are observed for the C4 and C5 atoms: 0.617(3) and 0.612(2) Å, respectively. Each CrPcI₂ molecule is bridged by a neutral I₂ molecule through the axially coordinated I atoms develop-

(24) Sheldrick, G. M. *SHELXL-97, Program for the Solution and Refinement of Crystal Structures*; University of Göttingen: Göttingen, Germany, 1997.

(25) Phillips, T. E.; Anderson, J. R.; Schramm, C. J.; Hoffman, B. M. *Rev. Sci. Instrum.* **1979**, *50*, 263–265.

(26) Mobaraki, B.; Ley, M.; Benlian, D.; Sorbier, J. P. *Acta Crystallogr.* **1990**, *C46*, 379–385.

(27) Janczak, J. *Pol. J. Chem.* **2000**, *74*, 157–162.

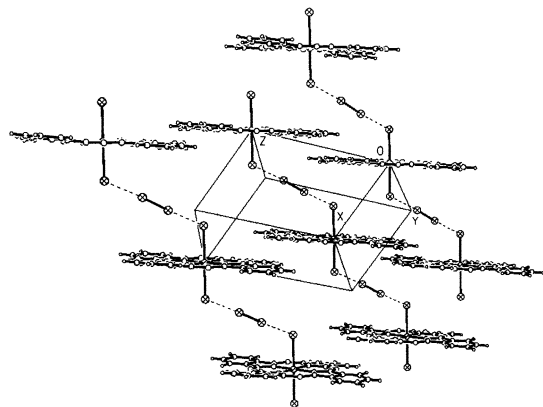


Figure 2. View of the chains of $(\text{CrPcI}_2 \cdot \text{I}_2)_n$ in the unit cell.

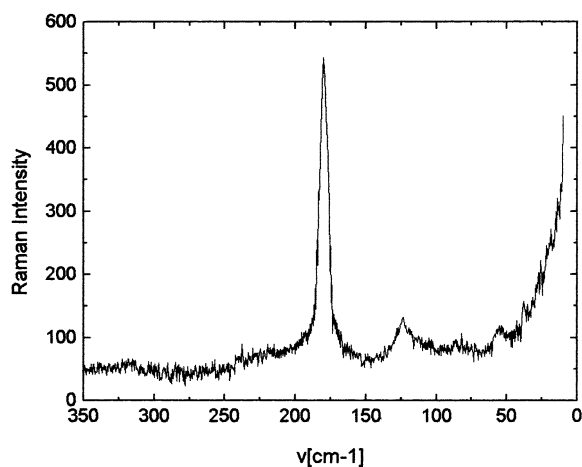


Figure 3. Resonance Raman spectrum of polycrystalline sample of $\text{CrPcI}_2 \cdot \text{I}_2$.

ing a one-dimensional zigzag polymeric structure (Figure 2). The $\text{Cr} \cdots \text{Cr}$ distance in the polymer is relatively very long ($12.942(3) \text{ \AA}$). The $\text{I}-\text{I}$ bond length in the bridging diiodine molecule, $2.773(1) \text{ \AA}$, is comparable to that found in the pure iodine (the $\text{I}-\text{I}$ bond length in pure iodine is equal to $2.715(6) \text{ \AA}$ at 110 K ²⁸). The $\text{I}-\text{I}$ bond distance in the present chromium complex provided evidence of the existence of neutral diiodine molecules in the crystal. The neutral diiodine molecule in the crystal has been also detected by Raman spectroscopy. The Raman spectrum (Figure 3) shows the expected vibrational band (at $\sim 180 \text{ cm}^{-1}$) of the I_2 molecule that interacts weakly with the axial I atoms of the CrPcI_2 molecules. This pattern is characteristic for the complexes containing the slightly interacting diiodine molecule.^{29,30} Relatively few structures have been reported for compounds having a neutral I_2 molecule coordinated between two iodine atoms,³¹ but only two are metallophthalocyanine structures: $\text{GePcI}_2 \cdot \text{I}_2$ in which the iodine molecules (with the $\text{I}-\text{I}$ distance of $2.770(2) \text{ \AA}$) similarly to this Cr complex develop a polymeric structure³² and $(\text{FePcI})_2 \cdot \text{I}_2$, in which the iodine

(28) Van Bolhuis, F.; Koster, B. P.; Mighelsen, T. *Acta Crystallogr.* **1967**, *23*, 90–93.

(29) (a) Teitebaum, R. C.; Ruby, S. L.; Marks, T. J. *J. Am. Chem. Soc.* **1978**, *100*, 3215–3217. (b) Teitebaum, R. C.; Ruby, S. L.; Marks, T. J. *J. Am. Chem. Soc.* **1980**, *102*, 3222–3228.

(30) Mizuno, M.; Tanaka, J.; Harada, I. *J. Phys. Chem.* **1981**, *85*, 1789–1794.

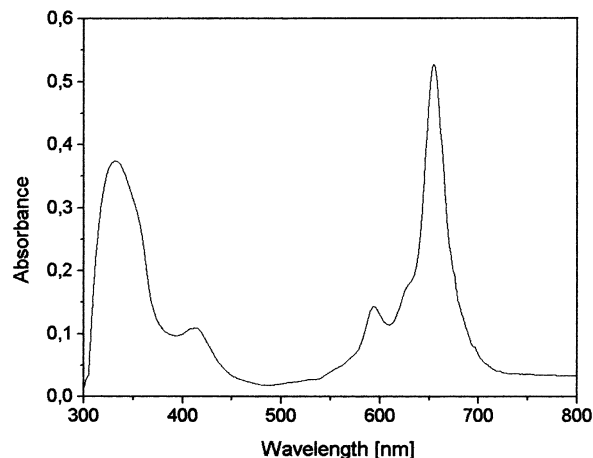


Figure 4. Electronic absorption spectrum of $\text{CrPcI}_2 \cdot \text{I}_2$ in dichloromethane.

molecule (with the distance of $2.766(2) \text{ \AA}$) is a bridge for dimerization of FePcI molecules.³³ A neutral diiodine molecule acting as a bridge can also be found in the iodine-doped chloro[phthalocyaninato(2-)]iron(III), $(\text{FePcI})_2 \cdot \text{I}_2$.³⁴ The $\text{I}-\text{I}$ distance of $3.502(1) \text{ \AA}$ between the axially coordinated I atoms and the bridging I_2 molecule in the chains indicates the interaction, which is comparable to the intermolecular interaction in pure iodine in the solid state (the $\text{I} \cdots \text{I}$ intermolecular distance in pure iodine is equal to 3.50 \AA).²⁸ The axial $\text{Cr}-\text{I}$ bond length of $2.750(1) \text{ \AA}$ is relatively long. In the series of the isostructural CrPcCl_2 , FePcCl_2 , and CoPcCl_2 complexes with the $\text{M}-\text{Cl}$ bond distances of $2.34(1)$, $2.260(1)$, and $2.261(1) \text{ \AA}$, respectively,²⁶ the longer $\text{Cr}-\text{Cl}$ bond distance in relation to $\text{Fe}-\text{Cl}$ and $\text{Co}-\text{Cl}$ is explained by the difference in the electron configuration of the central metal ions. According to the calculation performed by Whangbo and Stewart, the 3d electron energy is weaker in the CrPcCl_2 complex than in the FePcCl_2 or CoPcCl_2 complex, and less stabilizing of the overlap with the axial ligand.³⁵ In the present $\text{CrPcI}_2 \cdot \text{I}_2$ complex, the $\text{Cr}-\text{I}$ bond distance is additionally extended because of the $\text{I} \cdots \text{I}_2$ interaction that develops the polymeric structure.

UV–Vis Spectroscopy. The electronic absorption spectrum of $\text{CrPcI}_2 \cdot \text{I}_2$ complex in dichloromethane solution is shown in Figure 4. Several theoretical calculations for D_{4h} symmetry of the metallophthalocyanine molecule predict two distinct bands (B-Soret and Q) in the spectral region 300–800 nm.³⁶ The Q-band in the spectrum of $\text{CrPcI}_2 \cdot \text{I}_2$ in solution corresponds to the excitation from HOMO (a_{1u}) to

(31) (a) Tebbe, K. F.; Plewa, M. *Z. Anorg. Allg. Chem.* **1982**, *489*, 111. (b) Millan, A.; Bailey, P. M.; Maitlis, P. M. *J. Chem. Soc., Dalton Trans.* **1982**, 73–77. (c) Gray, L. R.; Gulliver, D. J.; Lewanson, W.; Webster, M. *Inorg. Chem.* **1983**, *22*, 2362–2366.

(32) Janczak, J.; Razik, M.; Kubiak, R. *Acta Crystallogr.* **1999**, *C55*, 359–361.

(33) Janczak, J.; Kubiak, R.; Hahn, F. *Inorg. Chim. Acta* **1999**, *287*, 101–104.

(34) Palmer, S. M.; Stanton, J. L.; Jaggi, N. K.; Hoffman, B. M.; Ibers, J. A. *Inorg. Chem.* **1985**, *24*, 2040–2046.

(35) Whangbo, M.; Stewart, K. R. *Isr. J. Chem.* **1983**, *23*, 113–138.

(36) (a) Schafer, A. M.; Gouterman, M. *Theor. Chim. Acta* **1972**, *27*, 62–68. (b) Mathur, S. C. *J. Chem. Phys.* **1968**, *45*, 3470–3472. (c) Zerner, M.; Gouterman, M. *Theor. Chim. Acta* **1966**, *4*, 44–63. (d) Schaffer, A. M.; Gouterman, M.; Davidson, E. R. *Theor. Chim. Acta* **1973**, *30*, 9–30.

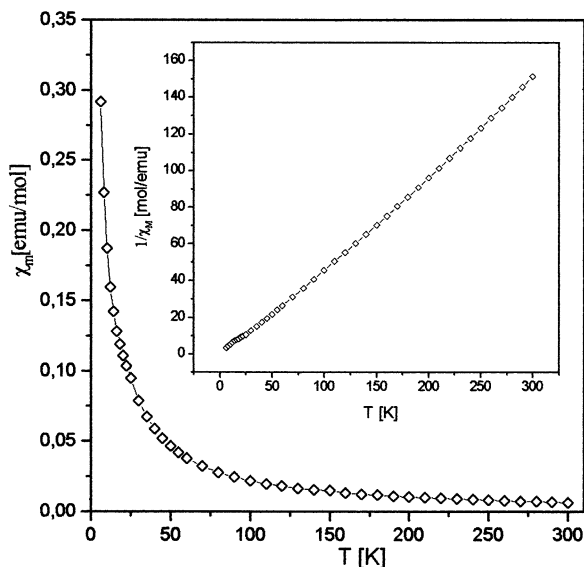


Figure 5. Plots of χ_M and $1/\chi_M$ of the $\text{CrPcI}_2 \cdot \text{I}_2$ solid sample versus T .

LUMO (e_g), while the B-band at ~ 335 nm is mostly an $a_{2u} \rightarrow e_g$ transition. The Q-band splits into two bands at ~ 655 and ~ 592 nm. The splitting value of the Q-band equals about 60 nm as a result of the vibronic coupling in the excited state.³⁷ For a comparison, for the vapor phase spectrum of CrPc {phthalocyaninato(2 $-$) chromium(II)} as well as for the same compound in DMSO solution, these characteristic B- and Q- bands (Q-splits) are observed at 315, 600, and 664 nm and 344, 622, and 685 nm, for vapor and in solution, respectively.³⁸ Besides these two characteristic bands (B and Q) observed in the spectrum of other metallophthalocyanines, one additional band at ~ 415 nm is observed in the spectrum of the $\text{CrPcI}_2 \cdot \text{I}_2$ complex. This band is evidence for the existence of the one-electron oxidized phthalocyaninato(1 $-$) radical ligand and is assigned to the electronic transition from a deeper level to the half-occupied HOMO level. A similar band has been observed in the spectrum of other one-electron oxidized metallophthalocyaninato complexes, such as LiPc , LnPc_2 , or InPc_2 .³⁹

Magnetic Properties. To understand the magnetic interactions between the central chromium(III) cation and the π -delocalized phthalocyaninato(1 $-$) radical, we performed magnetic susceptibility measurements on the polycrystalline sample in the temperature range from 300 to 2 K, and the results are shown in Figure 5. The thermal dependence of $1/\chi_M$ in the range 300–25 K is well fit by the Curie–Weiss law, $\chi_M = C/(T - \theta)$ with the θ constant -6.4 K. The effective magnetic moment was calculated by the relation $\mu_{\text{eff}} = 2.828(\chi_M T)^{1/2} \mu_B$. The effective magnetic moment calculated at room temperature is $3.98 \mu_B$. This value is

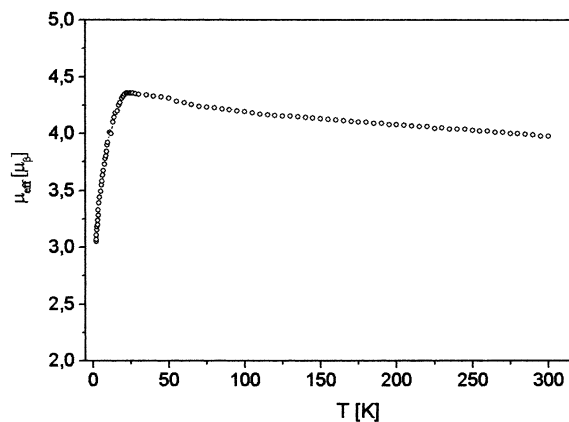


Figure 6. Temperature dependence of the effective magnetic moment, μ_{eff} , of $\text{CrPcI}_2 \cdot \text{I}_2$.

slightly higher than the spin-only magnetic moment for Cr^{3+} , $\mu_{\text{spin-only}} = 3.87 \mu_B$ (d^3 , $S = 3/2$), but it is considerably lower than that for the ferromagnetic coupling with the one-electron oxidized phthalocyaninato(1 $-$) radical ($S = 1/2$). The temperature dependence of the effective magnetic moment for $\text{CrPcI}_2 \cdot \text{I}_2$ is shown in Figure 6. As the temperature decreases in the range from 300 to 25 K, the μ_{eff} gradually increases to the value $4.36 \mu_B$. Below 25 K, the effective magnetic moment decreases more quickly and, at 2 K, is equal to $\sim 3.07 \mu_B$. The observed thermal behavior of the effective magnetic moment, μ_{eff} , indicates the quintet (300–25 K) and triplet (below 25 K) ground states, which might be produced by the ferro- and antiferromagnetic interactions between the paramagnetic Cr^{3+} central metal ion with the configuration of d^3 and $S = 3/2$ and the surrounding one-electron oxidized π -delocalized phthalocyaninato(1 $-$) radical ligand ($S = 1/2$). The EPR spectrum on the solid-state samples of $\text{CrPcI}_2 \cdot \text{I}_2$ at room temperature exhibits two signals. One sharp line at $g = 2.0020$ is attributed to the one-electron oxidized phthalocyaninato(1 $-$) radical macrocyclic ring. The g value of 2.0020 is close to the value of the free electron ($g = 2.0023$) and comparable to the value observed in the partially oxidized metallophthalocyaninato complexes.^{11–14,40} The other broad signal at $g \approx 1.96$ is attributed to the paramagnetic Cr^{3+} (d^3) central cation. This g value is typical for the hexacoordinated Cr(III) complexes (1.93–1.99) and indicates the localization of the electrons in the central chromium cation.⁴¹ The calculations of the spin concentrations yield 5.6×10^{20} spins/g (~ 0.96 unpaired electron per molecule) and 1.65×10^{21} spins/g (~ 2.93 unpaired electron per molecule) for the sharp line and broad signal, respectively. The EPR experiment indicates the slight interactions between the conducting electrons from the π -delocalized phthalocyaninato(1 $-$) ligand and the localized electrons on the central Cr cation. The natural abundance of ^{53}Cr with $I = 3/2$ is equal to $\sim 9.5\%$; however, the hyperfine structure of the EPR signal was not observed. This is typical for the species containing a very high spin concentration.

(37) (a) Henrikson, A.; Roos, B.; Sundon, R. *Theor. Chim. Acta* **1972**, *27*, 303–309. (b) Lee, L. K.; Sabelli, N. H.; Lebreton, P. R. *J. Phys. Chem.* **1982**, *86*, 3926–3931. (c) Shiari, H.; Tsuiki, H.; Masuda, E.; Koyama, T.; Hanabusa, K.; Kobayashi, N. *J. Phys. Chem.* **1991**, *95*, 417–423. (38) Edwards, L.; Gouterman, M. *J. Mol. Spectrosc.* **1970**, *33*, 292–310. (39) (a) Turek, P.; Andre, J. J.; Giraudeau, J.; Simon, J. *Chem. Phys. Lett.* **1987**, *134*, 471–476. (b) Sugimoto, H.; Higashi, T.; Mori, M. *J. Chem. Soc., Chem. Commun.* **1983**, 622–623. (c) Sugimoto, H.; Higashi, T.; Mori, M. *Chem. Lett.* **1983**, 1167–1169. (d) Ort, E.; Bredas, J. E.; Clarisse, C. *J. Chem. Phys.* **1990**, *92*, 1228–1235. (e) Janczak, J. *Pol. J. Chem.* **1998**, *72*, 1871–1878.

(40) Janczak, J.; Kubiak, R.; Jezierski, A. *Inorg. Chem.* **1995**, *34*, 3505–3509.

(41) Summerville, D. A.; Jones, R. D.; Hoffman, B. M.; Basolo, F. J. *J. Am. Chem. Soc.* **1977**, *99*, 8195–8202.

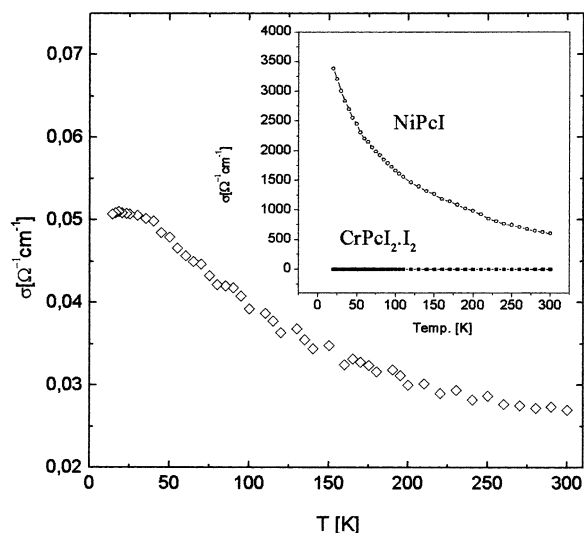


Figure 7. Temperature dependence of the conductivity of polycrystalline sample of $\text{CrPcI}_2 \cdot \text{I}_2$. Inset: comparison between the conductivities of NiPcI and $\text{CrPcI}_2 \cdot \text{I}_2$.

Conductivity Properties. The four-probe conductivity measurement of a polycrystalline sample of $\text{CrPcI}_2 \cdot \text{I}_2$ complex at room temperature is in the range $(2.7\text{--}2.8) \times 10^{-2} \Omega^{-1} \text{ cm}^{-1}$. Figure 7 shows very weak temperature dependence of the conductivity measured on a compacted polycrystalline sample over the range 300–15 K. There is a metallic-like dependence in conductivity, $d\sigma/dT < 0$, throughout the temperature range. At low temperature (15–30 K), a plateau in the conductivity is observed, which correlates with the change from the ferro- to antiferromagnetic coupling between the paramagnetic Cr^{3+} ions and the surrounding $\text{Pc}(1-)$ radical ligand observed in the magnetic susceptibility measurements. The electric behavior of the solid compound can be explained by the established structure. The one-dimensional arrangement of the CrPcI_2 molecules through the neutral I_2 molecules into a polymeric chain does not allow an efficient overlap between adjacent aromatic macrorings; the $\text{Pc} \cdots \text{Pc}$ distance in the polymeric chain of $9.287(3) \text{ \AA}$ is too long for effective π – π interactions. However, the $\text{Pc} \cdots \text{Pc}$ distance of $3.258(3) \text{ \AA}$ between two neighboring zigzag chains (see Figure 2) indicates the effective π – π interactions, because the distance is shorter than the van der Waals distance of 3.4 \AA for aromatic carbon atoms.⁴² On the other hand, the large $\text{Pc}(1-)$ radicals will allow intermolecular mobility of the electrons between the half-occupied π -levels. The rather weakly axially bound iodine atoms which interact with the relatively easy librating diiodine bridging molecule, for which the displacement thermal parameter, especially U_{33} for the I atoms of the I_2 molecule, is relatively great ($\sim 0.0871(3) \text{ \AA}^2$), would add a cooperative action to the process of electron hopping favored by the lattice fluctuations; hence, the rather high conductivity compares to the noniodinated metallophthalocyaninato complexes ($\sim 10^{-12}\text{--}10^{-10} \Omega^{-1} \text{ cm}^{-1}$).⁴³ The relatively high conductivity

observed for $\text{CrPcI}_2 \cdot \text{I}_2$ is comparable to that observed for CrPcCl_2 , FePcCl_2 , and CoPcCl_2 (room temperature conductivity $\sim 10^{-2}\text{--}10^{-3} \Omega^{-1} \text{ cm}^{-1}$), the three isostructural metallophthalocyaninato complexes which contain the one-electron oxidized phthalocyaninato(1 $-$) radical ligand,²⁶ but this does not give evidence for the intrinsic nature of the charge carriers. The metallic dependence of the conductivity has been also observed in the crystal of the oxomolybdenum(V) phthalocyaninato(2 $-$) triiodide complex in which the charge transport proceeds mainly along the pseudo-one-dimensional $(\text{MoOPcI}_3)_n$ aggregates.¹⁷ In some molecular conductors based on metallophthalocyanines such as $\text{TPP}[\text{Co}^{\text{III}}\text{Pc}(\text{CN})_2]_2$ and $\text{TPP}[\text{Fe}^{\text{III}}\text{Pc}(\text{CN})_2]_2$ (TPP = tetraphenylphosphonium cation) and in the neutral radical complexes $\text{Fe}^{\text{III}}\text{Pc}(1-)\text{Cl}_2 \cdot 2\text{CH}_3\text{COCH}_3$, $\text{Fe}^{\text{III}}\text{Pc}(1-)(\text{CN})_2 \cdot 2\text{CHCl}_3$, and $\text{Co}^{\text{III}}\text{Pc}(1-)(\text{CN})_2 \cdot 2\text{CHBr}_3$ in which the Pc-plane to Pc-plane distances are in the range $3.40\text{--}3.70 \text{ \AA}$, the relatively high electrical conductivity ($10^{-2}\text{--}10^{-3} \Omega^{-1} \text{ cm}^{-1}$) has also been observed.⁴⁴ Additionally, the interaction between the conduction electrons of the phthalocyaninato macrocycle and the localized magnetic spins on the central metal cation was suggested.⁴⁴ Metallic-like conductivity has been observed in the series of partially oxidized iodine-doped metallophthalocyaninato MPcI_x and diphthalocyaninato MPc_2I_x complexes. For example, the molecular conductor of NiPcI with the interplanar Pc–Pc spacing of 3.237 \AA exhibits the highest electrical conductivity ($\sigma_{\text{RT}} \approx 600 \Omega^{-1} \text{ cm}^{-1}$)⁴⁵ in this class of complexes where the charge transport is ligand-based, while in CoPcI partial oxidation occurs at the metal center rather than the ring, and the compound thus is a metal-spine conductor ($\sigma_{\text{RT}} \approx 65 \Omega^{-1} \text{ cm}^{-1}$).⁴⁶ This class of molecular conductors is isostructural with the characteristic interplanar spacing not too different from $\sim 3.25 \text{ \AA}$. Although, in the crystals of $\text{CrPcI}_2 \cdot \text{I}_2$, the interplanar Pc–Pc distance along the polymeric chain is relatively very long ($9.287(3) \text{ \AA}$), the Pc–Pc distance of $3.258(3) \text{ \AA}$ between the neighboring chains is comparable to that observed for the partially oxidized molecular conductors of MPcI as mentioned previously and indicates the effective π – π interaction between the phthalocyaninato(1 $-$) rings. Thus, the relatively high electrical conductivity is apparently due to the interchain π – π interactions of the phthalocyaninato(1 $-$) rings that overlap only partial, in contrast to the tetragonal conducting

(42) Pauling, L. *The Nature of the Chemical Bond*; Cornell University Press: Ithaca, NY, 1960; p 262.

(43) Gutman, F.; Lyone, L. E. *Organic Semiconductors*; Wiley: New York, 1967.

(44) (a) Inabe, T.; Maruyama, Y. *Bull. Chem. Soc. Jpn.* **1990**, *63*, 2273–2280. (b) Inabe, T.; Morimoto, K. *Synth. Met.* **1997**, *86*, 1779–1780. (c) Matsuda, M.; Naito, T.; Inabe, T.; Otsuka, T.; Awaga, K. *Synth. Met.* **1999**, *102*, 1774–1775. (d) Hasegawa, H.; Naito, T.; Inabe, T.; Akutagawa, T.; Nakamura, T. *J. Mater. Chem.* **1998**, *8*, 1567–1570. (e) Matsuda, M.; Naito, T.; Inabe, T.; Hanasaki, N.; Tajima, H.; Otsuka, T.; Awaga, K.; Narymbetov, B.; Kobayashi, H. *J. Mater. Chem.* **2001**, *10*, 631–636.

(45) (a) Petersen, J. L.; Schramm, C. J.; Stojakovic, D. R.; Hoffman, B. M.; Marks, T. J. *J. Am. Chem. Soc.* **1977**, *99*, 286–288. (b) Schramm, C. J.; Stojakovic, D. R.; Hoffman, B. M.; Marks, T. J. *Science* **1978**, *200*, 47–48. (c) Schramm, C. J.; Scaringe, R. P.; Stojakovic, D. R.; Hoffman, B. M.; Ibers, J. A.; Marks, T. J. *J. Am. Chem. Soc.* **1980**, *102*, 6702–6713. (d) Martinsen, J.; Palmer, S. M.; Tanaka, J.; Greene, R. L.; Hoffman, B. M. *Phys. Rev. B: Condens. Matter* **1984**, *30*, 6296–6276.

(46) Martinsen, J.; Stanton, J. L.; Jaggi, N. K.; Hoffman, B. M.; Ibers, J. A.; Schwartz, L. H. *J. Am. Chem. Soc.* **1985**, *107*, 83–91.

Magnetic Interactions in Metal–Radical System

materials of MPCl_x in which the whole π – π overlap is present.

Acknowledgment. This work was supported by the CNPq foundation.

Supporting Information Available: X-ray crystallographic file in CIF format. This material is available free of charge via the Internet at <http://pubs.acs.org>.

IC020258L